



## ORIGINAL ARTICLE

# Synthesis, molecular modelling and docking studies of new thieno[2,3-*b*:4,5-*b'*] dipyridine compounds as antimicrobial agents



Noof A. Alenazi<sup>a</sup>, Ahmad Fawzi Qarah<sup>b</sup>, Mansoor Alshahag<sup>c</sup>, Haifa Alharbi<sup>d</sup>, Abrar Bayazeed<sup>e</sup>, Salhah D. Al-Qahtani<sup>f</sup>, Nashwa M. El-Metwaly<sup>e,g,\*</sup>

<sup>a</sup> Department of Chemistry, College of Science and Humanities in Al-Kharj, Prince Sattam bin Abdulaziz University, Al-Kharj 11942, Saudi Arabia

<sup>b</sup> Department of Chemistry, College of Science, Taibah University, P.O. Box 344, Madinah, Saudi Arabia

<sup>c</sup> Department of Laboratory Medicine, Faculty of Applied Medical Sciences, Albaha University, Saudi Arabia

<sup>d</sup> Department of Chemistry, College of Science, Northern Border University, Saudi Arabia

<sup>e</sup> Department of Chemistry, Faculty of Applied Sciences, Umm Al-Qura University, Makkah, Saudi Arabia

<sup>f</sup> Department of Chemistry, College of Science, Princess Nourah bint Abdulrahman University, P.O. Box 84428, Riyadh 11671, Saudi Arabia

<sup>g</sup> Department of Chemistry, Faculty of Science, Mansoura University, El-Gomhoria Street, 35516, Egypt

Received 17 February 2023; accepted 19 March 2023

Available online 23 March 2023

## KEYWORDS

Thieno-dipyridine;  
DMF-DMA;  
DFT/B3LYP;  
*S. aureus*;  
Molecular docking

**Abstract** A series of substituted thieno[2,3-*b*:4,5-*b'*]dipyridine compounds were synthesized based on the reactions of 2-acetyl-3-aminothieno[2,3-*b*]pyridine derivative **1** with 1,3-bifunctional reagents (malononitrile, cyanoacetamide, acetylacetone, ethyl acetoacetate) and/or DMF-DMA. The frontier molecular orbitals of the produced derivatives were obtained from DFT/B3LYP calculations to investigate their structural and energetic properties. The data revealed that they had a low energy gap ( $\Delta E_{H-L}$ ), 2.32–3.39 eV, where compounds **3** and **6** displayed the smallest and greatest values, respectively. Meanwhile, the antibacterial activity of synthesized thieno[2,3-*b*:4,5-*b'*]dipyridine analogues was tested against four bacterial strains. Derivatives **2**, **3**, **5** and **8** exhibited good activity against Gram-positive bacteria rather than Gram-negative comparable to the ampicillin drug reference. Also, thienodipyridine analogues **2**, **3**, **5** and **8** displayed good activity in general, but against Gram-positive rather than Gram-negative bacteria. Meanwhile, the SAR of the synthesized analogues was discussed to describe the effect of their substituents on both two Gram-positive bacteria (*S. aureus* and *B. subtilis*) and two Gram-negative bacteria (*S. typhimurium* and *E. coli*). Also, the molecular docking estimation was applied on these hybrids to inspect their binding interactions toward the *E. coli* DNA gyrase B active site (PDB code: 1AJ6).

© 2023 The Author(s). Published by Elsevier B.V. on behalf of King Saud University. This is an open access article under the CC BY-NC-ND license (<http://creativecommons.org/licenses/by-nc-nd/4.0/>).

\* Corresponding author at: Department of Chemistry, Faculty of Applied Sciences, Umm Al-Qura University, Makkah, Saudi Arabia.  
E-mail address: [nmmohamed@uqu.edu.sa](mailto:nmmohamed@uqu.edu.sa) (N.M. El-Metwaly).

## 1. Introduction

Inspired the significant role of heterocycles in the pharmaceutical, agrochemical industries, and are intricately woven into life's fundamental processes (Bhargava et al., 2021). Over 90% of newly synthesized and commercialized pharmaceuticals have heterocyclic compounds, which have pharmacological, toxicological, physico-chemical, and pharmacokinetic effects (Adibpour et al., 2007, Koller et al., 2012). The synthesis of new compounds and subsequent evaluation of their biological activity was an empirical approach that gave rise to the field of medicinal chemistry (Al-Mulla, 2017, Fascio et al., 2015, Tevyashova and Chudinov, 2021). Owing to the qualities of its bioactivity, these pyridine moieties are essential in therapeutic chemistry. Since pyridine has a weak basicity, one of its uses in medical applications is to increase water solubility (Naushad and Thangaraj, 2022). Although greater water solubility has been a goal of many medications and pesticides with pyridine derivatives, this enhancement is frequently pH-dependent (Sun et al., 2022). For example, sulfapyridine has strong antibacterial effectiveness and water solubility in acidic medium, but there is a chance of crystallization in the urethra, which causes pain or urethral block (Fig. 1). Meanwhile, the conjugation between sulfapyridine and 5-aminosalicylic acid by an azo link affords sulfasalazine (Fig. 1). It exhibits better water solubility and is used in medical practice to cure Crohn's illness, colitis, and rheumatoid (Felson et al., 2011). If a pyridine ring cannot be added to the parent chemical structure, a water-soluble prodrug is an option.

The favorite thienopyridine ring found in a wide variety of prepared heterocyclic frames has been connected to a variety of bioactivities (Ul-Haq et al., 2020, Abuelhassan et al., 2022, Bakhite et al., 2003). They have distinctive and fascinating characteristics in the world of thiophene fused with six-membered pyridine structures. Medicinal chemists are increasingly turning to scaffolds to synthesize a variety of novel bioactive thienopyridine compounds, including anti-inflammatory, anti-infective, anti-depressant, antimicrobial, antiviral, and antiproliferative agents (Nakamura et al., 2017). Moreover, the thienopyridine moiety plays a significant molecular role in anti-aggregation drugs (Fig. 2). The first drug with in vitro anti-inflammatory (carrageenan-induced emphysema) and inhibition of ADP-induced platelet aggregation activity was ticlopidine, a tetrahydrothieno[3,2-*c*]pyridine derivative, clopidogrel, which has the same ring, and still available for use (Istanbullu et al., 2022). From the previous scientific literature, we go over how to make a couple brand-new thieno[2,3-*b*:4,5-*b'*]dipyridine analogues. Additionally, to theoretical estimation like molecular modelling and docking, the synthesized compounds were examined for both Gram-positive and Gram-negative bacterial strains.

## 2. Experimental

### 2.1. Materials and methods

Melting points were determined on an Electrothermal 9100 instrument. The IR spectra (KBr discs) were captured by a

Thermo Scientific's Nicolet iS10 FTIR spectrometer. Using a spectrometer manufactured by JEOL,  $^1\text{H}$  NMR (500 MHz) and  $^{13}\text{C}$  NMR (125 MHz) spectra were recorded in  $\text{DMSO-}d_6$ . Mass analyses were recorded by a Quadrupole GC-MS (DSQII) mass spectrometer at a setting of 70 eV. Elemental analyses were determined using a Perkin-Elmer 2400 analyzer (C, H, and N).

### 2.2. Synthesis of 2-amino-4,7,9-trimethyl-3-substituted-thienodipyridines 2 and 3

A mixture of 2-acetyl-3-aminothienopyridine compound **1** (0.88 g, 4 mmol) and malononitrile (0.27 g, 4 mmol) or cyanoacetamide (0.34 g, 4 mmol) in sodium ethoxide solution (prepared from 0.14 g sodium metal and 30 mL absolute ethanol) was refluxed for 4 h. The mixture was poured into ice-cold water and neutralized by dilute HCl. The separated solid was collected and crystallized from ethanol to furnish the corresponding thieno-dipyridine compounds **2** and **3**, respectively.

#### 2.2.1. 2-Amino-3-cyano-4,7,9-trimethylthieno[2,3-*b*:4,5-*b'*]dipyridine (2)

Light green powder; yield = 68%; m.p. = 245–246 °C. IR ( $\bar{\nu}/\text{cm}^{-1}$ ): 3360, 3294 ( $-\text{NH}_2$ ), 2212 ( $\text{C}\equiv\text{N}$ ), 1649 ( $\text{C}=\text{N}$ ).  $^1\text{H}$  NMR ( $\delta/\text{ppm}$ ): 2.32 (s, 3H,  $-\text{CH}_3$ ), 2.42 (s, 3H,  $-\text{CH}_3$ ), 2.71 (s, 3H,  $-\text{CH}_3$ ), 7.04 (s, 1H, C5-pyridine), 7.12 (s, 2H,  $-\text{NH}_2$ ).  $^{13}\text{C}$  NMR ( $\delta/\text{ppm}$ ): 15.82 ( $-\text{CH}_3$ ), 19.13 ( $-\text{CH}_3$ ), 24.04 ( $-\text{CH}_3$ ), 87.43, 113.60 ( $-\text{C}\equiv\text{N}$ ), 122.74, 124.33, 126.56, 144.59, 151.62, 156.91, 159.78, 161.17, 161.86. MS (EI,  $m/z$ ): 268 (13.32%). Anal. Calcd. for  $\text{C}_{14}\text{H}_{12}\text{N}_4\text{S}$  (268.08): C, 62.66; H, 4.51; N, 20.88%. Found: C, 62.76; H, 4.48; N, 20.93%.

#### 2.2.2. 2-Amino-4,7,9-trimethylthieno[2,3-*b*:4,5-*b'*]dipyridine-3-carboxamide (3)

Lemon powder; yield = 74%; m.p. = 263–264 °C. IR ( $\bar{\nu}/\text{cm}^{-1}$ ): 3338, 3288, 3214 ( $-\text{NH}_2$ ), 1657 (amide,  $\text{C}=\text{O}$ ).  $^1\text{H}$  NMR ( $\delta/\text{ppm}$ ): 2.31 (s, 3H,  $-\text{CH}_3$ ), 2.40 (s, 3H,  $-\text{CH}_3$ ), 2.68 (s, 3H,  $-\text{CH}_3$ ), 6.48 (s, 2H,  $-\text{NH}_2$ ), 7.05 (s, 1H, C5-pyridine), 7.87 (s, 2H,  $-\text{NH}_2$ ).  $^{13}\text{C}$  NMR ( $\delta/\text{ppm}$ ): 15.76 ( $-\text{CH}_3$ ), 19.22 ( $-\text{CH}_3$ ), 23.96 ( $-\text{CH}_3$ ), 115.07, 123.01, 124.40, 125.83, 144.47, 147.39, 155.58, 157.11, 159.65, 160.93, 166.35 ( $\text{C}=\text{O}$ ). MS (EI,  $m/z$ ): 286 (43.08%). Anal. Calcd. for  $\text{C}_{14}\text{H}_{14}\text{N}_4\text{O}_2\text{S}$  (286.09): C, 58.72; H, 4.93; N, 19.57%. Found: C, 58.87; H, 4.88; N, 19.50%.

### 2.3. Synthesis of 2,4,7,9-tetramethyl-3-substituted-thienodipyridines 4 and 5

A mixture of 2-acetyl-3-aminothienopyridine compound **1** (0.88 g, 4 mmol) and acetylacetone (0.40 g, 4 mmol) or ethyl

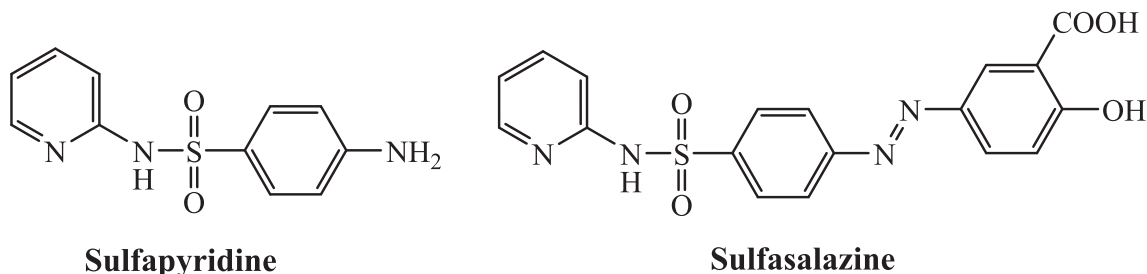
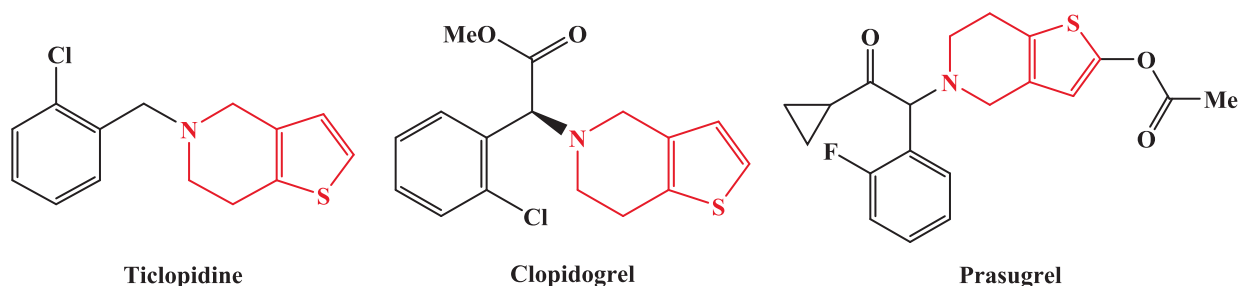


Fig. 1 Chemical structures of sulfapyridine and sulfasalazine.



**Fig. 2** Some of heterocyclic drugs containing thienopyridine moiety.

acetoacetate (0.52 g, 4 mmol) in sodium ethoxide solution (prepared from 0.14 g sodium metal and 30 mL absolute ethanol) was refluxed for 4 h. The mixture poured into ice-cold water and neutralized by dilute HCl. The solid that formed was collected and crystallized from ethanol to give the corresponding thieno-dipyridine compounds **4** and **5**, respectively.

#### 2.3.1. 3-Acetyl-2,4,7,9-tetramethylthieno[2,3-b:4,5-b']dipyridine (**4**)

Orange powder; yield = 63%; m.p. = 218–219 °C. IR ( $\bar{\nu}/\text{cm}^{-1}$ ): 1680 (C=O), 1633 (C=N).  $^1\text{H}$  NMR ( $\delta/\text{ppm}$ ): 2.19 (s, 3H, CH<sub>3</sub>), 2.35 (s, 3H), 2.51 (s, 3H, —CH<sub>3</sub>), 2.57 (s, 3H, —CH<sub>3</sub>), 2.69 (s, 3H, —CH<sub>3</sub>), 7.11 (s, 1H, C5-pyridine).  $^{13}\text{C}$  NMR ( $\delta/\text{ppm}$ ): 16.70 (—CH<sub>3</sub>), 18.96 (—CH<sub>3</sub>), 22.39 (—CH<sub>3</sub>), 23.81 (—CH<sub>3</sub>), 28.56 (COCH<sub>3</sub>), 122.89, 124.25, 127.26, 134.77, 143.39, 144.42, 156.11, 157.00, 159.53, 163.48, 193.20 (C=O). MS (EI,  $m/z$ ): 284 (30.53%). Anal. Calcd. for C<sub>16</sub>H<sub>16</sub>N<sub>2</sub>OS (284.10): C, 67.58; H, 5.67; N, 9.85%. Found: C, 67.40; H, 5.74; N, 9.74%.

#### 2.3.2. Ethyl 2,4,7,9-tetramethylthieno[2,3-b:4,5-b']dipyridine-3-carboxylate (**5**)

Orange powder; yield = 58%; m.p. = 230–231 °C. IR ( $\bar{\nu}/\text{cm}^{-1}$ ): 1714 (C=O), 1644 (C=N).  $^1\text{H}$  NMR ( $\delta/\text{ppm}$ ): 1.31 (t,  $J = 7.00$  Hz, 3H, —OCH<sub>2</sub>CH<sub>3</sub>), 2.38 (s, 3H, —CH<sub>3</sub>), 2.53 (s, 3H, —CH<sub>3</sub>), 2.68 (s, 3H, —CH<sub>3</sub>), 2.87 (s, 3H, —CH<sub>3</sub>), 4.26 (q,  $J = 7.00$  Hz, 2H, —OCH<sub>2</sub>CH<sub>3</sub>), 6.88 (s, 1H, C5-pyridine).  $^{13}\text{C}$  NMR ( $\delta/\text{ppm}$ ): 14.23 (—OCH<sub>2</sub>CH<sub>3</sub>), 16.56 (—CH<sub>3</sub>), 18.90 (—CH<sub>3</sub>), 22.25 (—CH<sub>3</sub>), 23.87 (—CH<sub>3</sub>), 60.94 (—OCH<sub>2</sub>CH<sub>3</sub>), 122.26, 122.83, 124.32, 126.97, 143.04, 144.61, 156.19, 156.87, 159.44, 161.31, 166.36 (C=O). MS (EI,  $m/z$ ): 314 (27.14%). Anal. Calcd. for C<sub>17</sub>H<sub>18</sub>N<sub>2</sub>O<sub>2</sub>S (314.11): C, 64.94; H, 5.77; N, 8.91%. Found: C, 65.11; H, 5.71; N, 8.84%.

#### 2.4. Synthesis of 4-hydroxy-7,9-dimethylthieno[2,3-b:4,5-b']dipyridine compounds **6** and **8**

To a solution of thienopyridine compound **1** and/or **7** (3 mmol) in 30 mL xylene, DMF-DMA (0.36 mL, 3 mmol) was added. The solution was subjected to reflux for 4 h. The solid that obtained upon cooling was collected and crystallized from EtOH to furnish the targeting 4-hydroxy-thieno[2,3-b:4,5-b']dipyridine compounds **6** and **8**, respectively.

##### 2.4.1. 4-Hydroxy-7,9-dimethylthieno[2,3-b:4,5-b']dipyridine (**6**)

Reddish brown powder; yield = 60%; m.p. = 284–285 °C. IR ( $\bar{\nu}/\text{cm}^{-1}$ ): 3161 (O—H), 1641 (C=N).  $^1\text{H}$  NMR ( $\delta/\text{ppm}$ ): 2.59

(s, 3H, —CH<sub>3</sub>), 2.78 (s, 3H, —CH<sub>3</sub>), 6.70 (d,  $J = 11.00$  Hz, 1H, C3-pyridine), 6.91 (s, 1H, C5-pyridine), 8.17 (d,  $J = 11.00$  Hz, 1H, C2-pyridine), 11.15 (s, 1H, O—H).  $^{13}\text{C}$  NMR ( $\delta/\text{ppm}$ ): 19.11 (—CH<sub>3</sub>), 24.02 (—CH<sub>3</sub>), 103.05, 115.81, 122.70, 124.39, 144.54, 151.98, 157.15, 159.48, 160.08, 163.69. MS (EI,  $m/z$ ): 230 (65.37%). Anal. Calcd. for C<sub>12</sub>H<sub>10</sub>N<sub>2</sub>OS (230.05): C, 62.59; H, 4.38; N, 12.16%. Found: C, 62.46; H, 4.34; N, 12.08%.

##### 2.5. Ethyl 4-hydroxy-7,9-dimethylthieno[2,3-b:4,5-b']dipyridine-3-carboxylate (**8**)

Reddish brown powder; yield = 56%; m.p. = 302–303 °C. IR ( $\bar{\nu}/\text{cm}^{-1}$ ): 3174 (O—H), 1667 (C=O), 1638 (C=N).  $^1\text{H}$  NMR ( $\delta/\text{ppm}$ ): 1.29 (t,  $J = 7.00$  Hz, 3H, —OCH<sub>2</sub>CH<sub>3</sub>), 2.55 (s, 3H, —CH<sub>3</sub>), 2.71 (s, 3H, —CH<sub>3</sub>), 4.23 (q,  $J = 7.00$  Hz, 2H, —OCH<sub>2</sub>CH<sub>3</sub>), 6.89 (s, 1H, C5-pyridine), 8.73 (s, 1H, C2-pyridine), 14.62 (s, 1H, O—H).  $^{13}\text{C}$  NMR ( $\delta/\text{ppm}$ ): 14.27 (—OCH<sub>2</sub>CH<sub>3</sub>), 19.06 (—CH<sub>3</sub>), 23.94 (—CH<sub>3</sub>), 60.88 (—OCH<sub>2</sub>CH<sub>3</sub>), 111.85, 115.73, 122.72, 124.27, 144.47, 152.03, 157.29, 159.38, 160.15, 163.51, 165.64 (C=O). MS (EI,  $m/z$ ): 302 (41.29%). Anal. Calcd. for C<sub>15</sub>H<sub>14</sub>N<sub>2</sub>O<sub>3</sub>S (302.07): C, 59.59; H, 4.67; N, 9.27%. Found: C, 59.76; H, 4.60; N, 9.38%.

#### 2.6. Computational calculations

Geometrical optimization of the synthesized thieno-dipyridine derivatives was carried out by the Gaussian 09W program (Frisch et al., 2009) at DFT/B3LYP/6-311<sup>++</sup>G(d,p) methodology (Becke, 1993, Lee et al., 1988, Perdew and Wang, 1992). The resulting electronic and frontier molecular orbitals of the optimized structures have been obtained using the GaussView program (Dennington et al., 2009). The B3LYP/DNP (version 3.5) method in the DMol3 module of Materials Studio software (BIOVIA, 2017) was applied in estimating the Fukui indices (Delley, 2006).

#### 2.7. Antimicrobial assay

The antibacterial procedure that was utilized in the study of the synthesized thieno-dipyridines is the agar disc-diffusion assay (Azoro, 2002, Al-Anazi et al., 2019, Kaushal et al., 2018). Gram-positive and Gram-negative microorganisms “*Bacillus subtilis* MTCC-5981, *Staphylococcus aureus* MTCC-740, *Escherichia coli*, *Salmonella typhimurium*, and *Pseudomonas aeruginosa* MTCC-424” are used in the testing. By sub-culturing microorganisms at 37 °C into microbial inoculums for 18 h, the bacteria were extracted. A 100 mL portion

of every test microorganism was moved to the sterilised Petri dishes. The experimental findings are reported as a mean standard deviation because they were performed in triplicate (SD). After 24 h, the inhibition zone diameters (IZD) were evaluated in duplicate experiments. The antibacterial ability of the synthesized thieno-dipyridines toward the examined pathogens was assessed using the IZD assay in comparison to the reference antibiotic Ampicillin. In contrast, all experiments were carried out using the solvent DMSO, which has no inhibitory activity. Meanwhile, minimum inhibitory concentration (MIC) values of thieno[2,3-*b*:4,5-*b'*] dipyridine hybrids were specified using agar dilution bacterial cultures and mentioned in the [supplementary file \(Al-Anazi et al., 2019\)](#).

### 2.8. Molecular docking (MD)

M.O.E “2015.10” program was used to carry out the molecular docking exploration. The Protein Data Bank was used to locate the structure of “*E. coli* topoisomerase II DNA gyrase B” (PDB: 1AJ6) ([Mohi El-Deen et al., 2019](#)). To calculate a root-mean-square deviation value, the co-crystallized ligands were initially redocked inside the designated active “*E. coli* DNA gyrase B” enzyme, ignoring heteroatoms and water, docking ligand atoms at the proper sites using 10 poses, optimization, and the ligands were docked. Following a previously described process, the newly synthesized thieno-dipyridines (**2**, **3**, **4**, **5**, **6**, and **8**) were molecularly docked inside the ATP-binding position of “*E. coli* DNA gyrase B” (PDB: 1AJ6).

## 3. Results and discussion

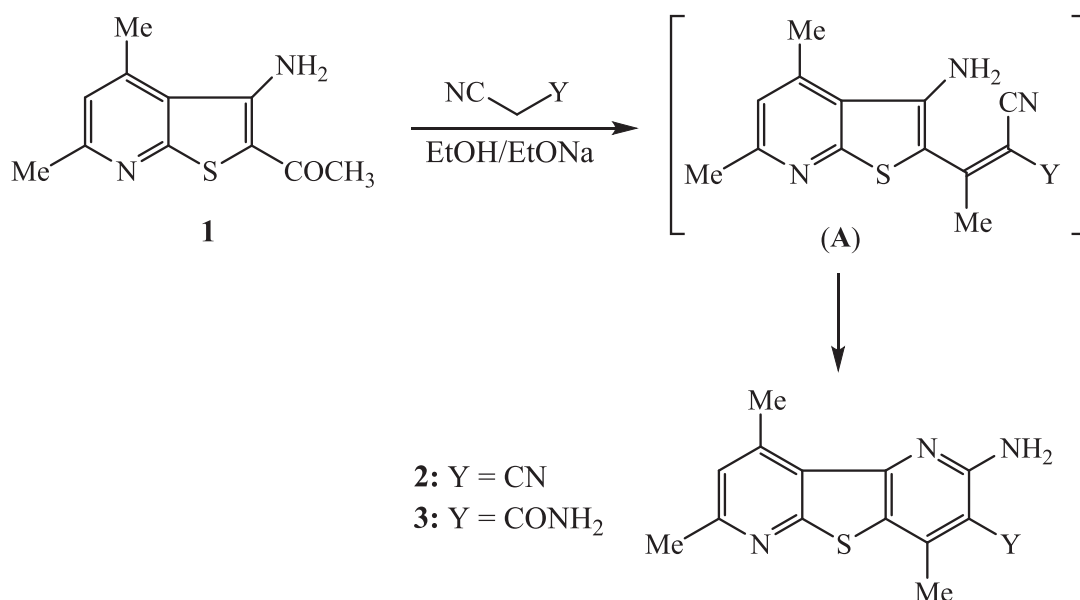
### 3.1. Chemistry

The first goal of this study involves exploration the synthetic potentially of 2-acetyl-3-amino-4,6-dimethylthieno[2,3-*b*]pyridine (**1**) ([Yassin, 2009](#)) via its reaction with active methylene compounds. Thus, the thienopyridine compound **1** was reacted

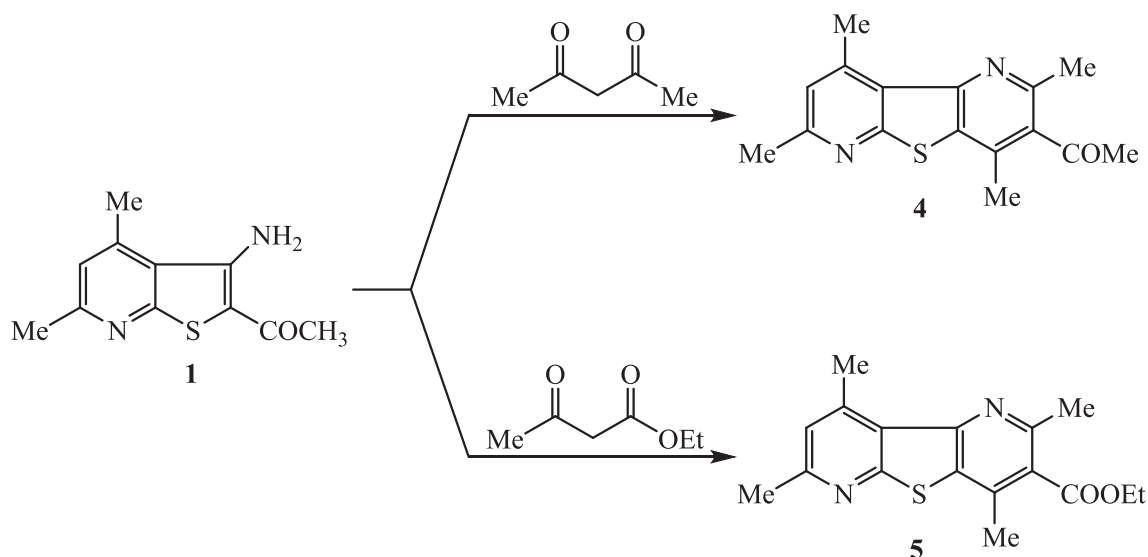
with activated nitriles (namely, malononitrile and cyanoacetamide) in refluxing ethanol/sodium ethoxide solution to give 3-(3-amino-4,6-dimethylthieno[2,3-*b*]pyridin-2-yl)but-2-enitrile intermediate (**A**) formed via the loss of water molecule followed by intramolecular cyclization to afford 2-amino-4,7,9-trimethylthieno[2,3-*b*:4,5-*b'*]dipyridine compounds **2** and **3** as sole product in each case ([Scheme 1](#)). The structure of thieno-dipyridine compounds **2** and **3** were established based on the data of their spectral analyses. The IR spectrum of compound **2** lacked an absorption band of C=O group and displayed bands at 3360, 3294 and 2212 for  $\text{—NH}_2$  and  $\text{—C}\equiv\text{N}$  groups, respectively. The  $^1\text{H}$  NMR spectrum of **2** revealed singlet signals at  $\delta$  2.32, 2.42, and 2.71 for the protons of three methyl groups. The protons of pyridine-C5 and amino ( $\text{—NH}_2$ ) were recorded as singlet signals at  $\delta$  7.04 and 7.12 ppm, respectively. The mass spectrum showed the expected molecular ion peak  $\text{M}^+$  at  $m/z$  268 (13.32%) for the formula  $\text{C}_{14}\text{H}_{12}\text{N}_4\text{S}$ .

In addition, treatment of thienopyridine compound **1** with acetylacetone and/or ethyl acetoacetate in boiling sodium ethoxide solution was the synthetic route for the production of 2,4,7,9-tetramethylthieno[2,3-*b*:4,5-*b'*]dipyridine derivatives **4** and **5**, respectively ([Scheme 2](#)). The IR spectrum of thienodipyridine analogue **4** exhibited the absorption of acetyl-carbonyl group at  $1680 (\text{C}=\text{O}) \text{ cm}^{-1}$ . The  $^1\text{H}$  NMR spectrum of thieno-dipyridine analogue **4** showed five singlet signals at  $\delta$  2.19, 2.35, 2.51, 2.57 and 2.69 ppm for the protons of five methyl groups. The proton of pyridine-C5 was recorded as singlet  $\delta$  7.11 ppm. The mass analysis of thieno-dipyridine analogue **4** showed the molecular ion peak at  $m/z$  284 ( $\text{M}^+$ , 30.53%) referring to the formula  $\text{C}_{16}\text{H}_{16}\text{N}_2\text{O}_2\text{S}$ .

The reaction of 2-acetyl-3-aminothieno[2,3-*b*]pyridine derivative **1** with DMF-DMA in boiling xylene did not stop at the intermediate (**A**) which undergoes intramolecular elimination of dimethylamine molecule. Aromaticity was the driving force behind intermediate (**B**) to furnish the final product, 4-hydroxythieno[2,3-*b*:4,5-*b'*]dipyridine compound **6** ([Scheme 3](#)) ([Mohamed et al., 2018](#), [Atta and Abdel-Latif,](#)



**Scheme 1** Synthesis of 2-aminothieno[2,3-*b*:4,5-*b'*]dipyridine derivatives **2** and **3**.



**Scheme 2** Synthesis of 2,4,7,9-tetramethylthieno[2,3-*b*:4,5-*b'*]dipyridine derivatives **4** and **5**.

2021). The IR spectrum exhibited absorptions at 3161 and 1641  $\text{cm}^{-1}$  that are ascribed to the stretching vibrations of hydroxyl (O—H) and imine (C=N) functions, respectively. The  $^1\text{H}$  NMR spectrum displayed two singlet signals at  $\delta$  2.59 (pyridine-CH<sub>3</sub>) and 2.78 ppm (pyridine-CH<sub>3</sub>). The protons of pyridine ring (C3 and C2) were observed as two double signals at  $\delta$  6.70 and 8.17 ppm, respectively. The protons of pyridine-C5 and hydroxyl group were observed as singlet signals at  $\delta$  6.91 and 11.15 ppm, respectively. The mass analysis indicated a molecular ion peak at  $m/z$  230 ( $\text{M}^+$ , 65.37%) corresponding to the formula  $\text{C}_{12}\text{H}_{10}\text{N}_2\text{OS}$ .

The reaction of ethyl 3-(3-amino-4,6-dimethylthieno[2,3-*b*]pyridin-2-yl)-3-oxopropanoate (**7**) (Rodinovskaya and Shestopalov, 2000) with DMF-DMA in boiling xylene did not stop at the intermediate (**C**) which undergoes intramolecular elimination of dimethylamine molecule followed by tautomerization of the produced intermediate (**D**) into the tricyclic ring system, 4-hydroxythieno[2,3-*b*:4,5-*b'*]dipyridine compound **8** (Scheme 4). The IR spectrum showed the absorptions of hydroxyl (O—H) and ester-carbonyl (C=O) functions at 3174 and 1667  $\text{cm}^{-1}$ . The  $^1\text{H}$  NMR spectrum identified the protons of ethoxy group (COOCH<sub>2</sub>CH<sub>3</sub>) as triplet and quartet at  $\delta$  1.29 and 4.23 ppm. The protons of two methyl groups were observed as singlet signals at  $\delta$  2.55 and 2.17 ppm. The protons of pyridine ring systems were recorded at  $\delta$  6.89 and 8.73 ppm. The proton of hydroxyl group was recorded as singlet at 14.62 ppm.

### 3.2. Computational studies

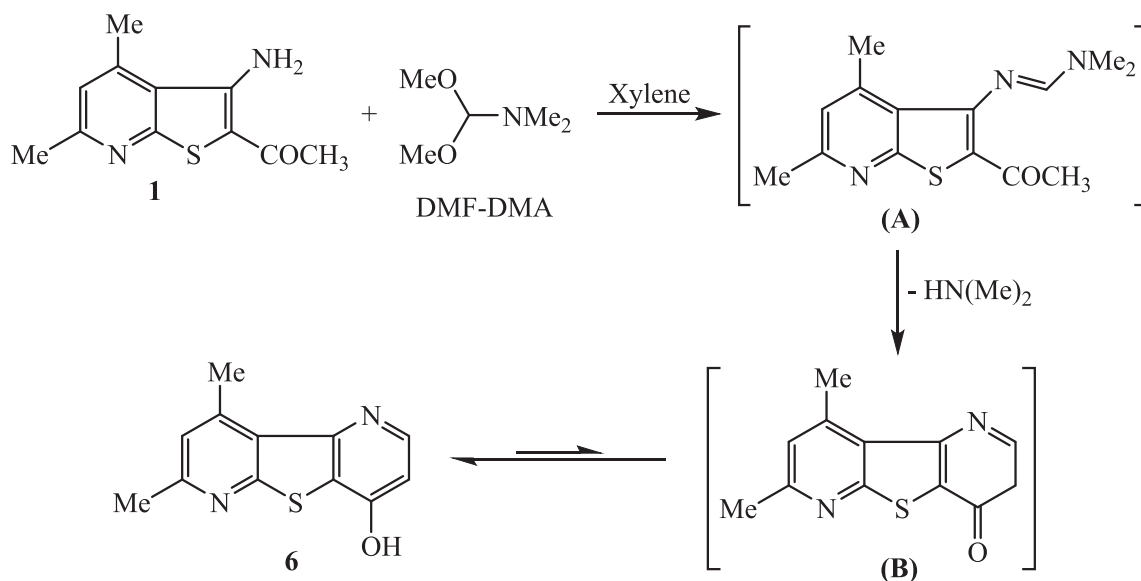
The DFT calculations of the thieno[2,3-*b*:4,5-*b'*]dipyridine derivatives, **2–8**, revealed that they have planar structures, with dihedral angles of 0.0° and/or 180.0° (Fig. 3). Whereas, in compound **3**, the obtained dihedral angle disclosed that the amide and amino groups were lying out the plane of the thienodipyridine moiety where, for example, the  $\text{CO}_{(\text{amd})}-\text{C}_{(\text{tpy})}^3-\text{N}_{(\text{tpy})}^1 = 172.8^\circ$ ,  $\text{C}_{(\text{tpy})}^2-\text{C}_{(\text{tpy})}^3-\text{CO}_{(\text{amd})}-\text{OC}_{(\text{amd})} = 19.8^\circ$ ,  $\text{C}_{(\text{tpy})}^2-\text{C}_{(\text{tpy})}^3-\text{CO}_{(\text{amd})}-\text{NH}_{2(\text{amd})} = -157.8^\circ$  and  $\text{CO}_{(\text{amd})}-\text{C}_{(\text{tpy})}^3-\text{C}_{(\text{tpy})}^2-\text{NH}_2 = -7.1^\circ$ . Likewise, in compound **4**, the

acetyl group has been departed the planarity as the  $\text{CO}_{(\text{Actl})}-\text{C}_{(\text{tpy})}^3-\text{C}_{(\text{tpy})}^2-\text{N}_{(\text{tpy})}^1 = 177.1$ ,  $\text{C}_{(\text{tpy})}^2-\text{C}_{(\text{tpy})}^3-\text{CO}_{(\text{Actl})}-\text{OC}_{(\text{Actl})} = 35.6$  and  $\text{C}_{(\text{tpy})}^2-\text{C}_{(\text{tpy})}^3-\text{CO}_{(\text{Actl})}-\text{Me}_{(\text{Actl})} = -140.2$  (Tables S1–S3).

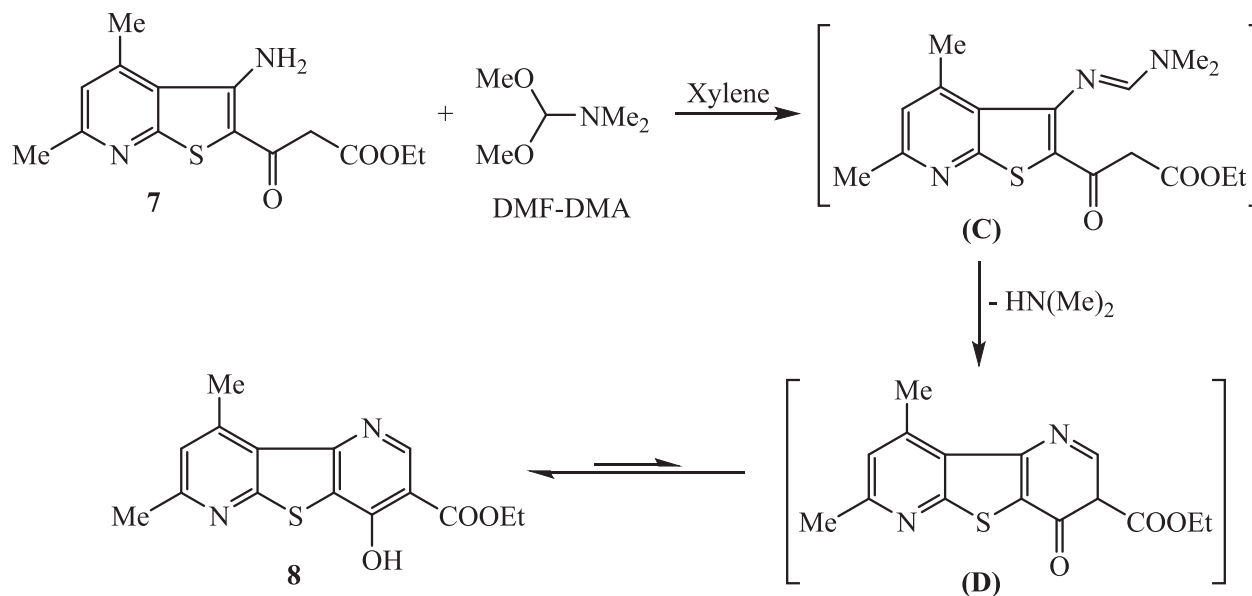
Moreover, the structural parameters, i.e., bond length and angle, displayed notable matching with the single crystal X-ray values of analogue derivatives (Klemm et al., 2000), where the lengths presented 0.16 Å maximum difference from the equivalent x-ray, RMSD 5.02–5.49  $\times 10^{-2}$ , while the differences of angles were 0.0–12.1°, RMSD = 4.36–4.86. Such differences might arise from the fact that no intermolecular columbic interactions take place in the quantum calculations because they involve a single gaseous molecule, whereas the actual information was gained from solid interacting molecules in crystal (Sajan et al., 2011) (Tables S1–S3).

The HOMO-LUMO shape and energy plays important role in empathizing the molecule's electrons donation and acceptance abilities (Bulat et al., 2004). The molecule's bioactivity may be influenced by HOMO-LUMO charge transfer, which becomes easier when the energy gap is reduced (Xavier et al., 2015, Makhlof et al., 2018, Bouchoucha et al., 2018). The HOMO of the **2–8** derivatives was chiefly made of the  $\pi$ -orbitals and heteroatoms non-bonding lone pairs of electrons of the thienodipyridine ring along with those of the substituent groups except the ester group in **5** and **8** compounds, while, their LUMO were built principally of the whole molecule  $\pi^*$ -orbitals (Fig. 4). The close configuration of HOMO-LUMO affected on the values of their energy,  $E_H$  and  $E_L$  (Table 1). For instance, the studied compounds offered  $E_H$  values from -6.43 eV for **8** to -5.67 eV for **3**, as well as, the  $E_L$  values were from -3.68 to -2.91 eV and accordingly sorted as **6** < **3** < **5** < **2** < **8** < **4**. Similarly, the considered compounds offered close and small gap ( $\Delta E_{H-L}$ ), 2.32–3.39 eV, and may be sorted as **3** < **2** < **4** < **8** < **5** < **6**. As a result, the 2-amino derivatives revealed a lower gap than the methyl and hydroxyl compounds (Table 1).

As well, some chemical reactivity descriptors, such as electronegativity ( $\chi$ ), global hardness ( $\eta$ ), softness ( $\delta$ ), electrophilicity ( $\omega$ ), electron-donating power ( $\omega^-$ ) and electron-



**Scheme 3** Synthesis of 4-hydroxythieno[2,3-*b*:4,5-*b'*]dipyridine compound **6**.



**Scheme 4** Synthesis of ethyl 4-hydroxy-thieno[2,3-*b*:4,5-*b'*]dipyridine-3-carboxylate compound **8**.

accepting power ( $\omega^+$ ) were calculated using the  $E_H$  and  $E_L$  as follows (Xavier et al., 2015).

$$\chi = -\frac{1}{2}(E_{HOMO} + E_{LUMO}) \quad \eta = -\frac{1}{2}(E_{HOMO} - E_{LUMO}) \quad \delta = \frac{1}{\eta}$$

$$\omega = \frac{z^2}{8\eta} \quad \omega^- = \frac{(3I+A)^2}{16(I-A)} \quad \omega^+ = \frac{(I+3A)^2}{16(I-A)}$$

As shown in Table 1, the compound **3** was the most chemically reactive, lowest kinetically stable and softest derivative where it exhibited the lowest global hardness ( $\eta$ ) and highest softness ( $\delta$ ) values. According to electrophilicity index ( $\omega$ ) which evaluate the stabilization energy of acquiring additional electronic charge from the environment, organic molecules with  $\omega > 1.5$  eV were ascribed as strong electrophile (Afolabi et al., 2022, Domingo et al., 2016). Thus, the studied com-

pounds were strong electrophile as they exhibited  $\omega$  index ranged from 1.56 to 2.34 eV following the order **6** < **5** < **3** < **2** < **8** < **4**. Likewise, the electron donating ( $\omega^+$ ) and acceptance ( $\omega^-$ ) powers of the investigated derivatives, which demonstrated the capability to give and receive electrons, respectively, obeyed the pervious order but they exhibited more donating power, 4.16–7.02 eV, than acceptance one, 8.76–12.06 eV, where smaller values signify enhanced transaction (Afolabi et al., 2022, Domingo et al., 2016) (Table 1).

Moreover, the Mulliken's atomic charges afforded a respectable interpretation of molecule's electronegativity and charge transfer (Bhagyasree et al., 2013). The investigated compounds atomic charges revealed that the thienodipyridine nitrogen's,  $N_{(tpy)}^1$  and  $N_{(tpy)}^6$ , had a positive charge, 0.022–0.376

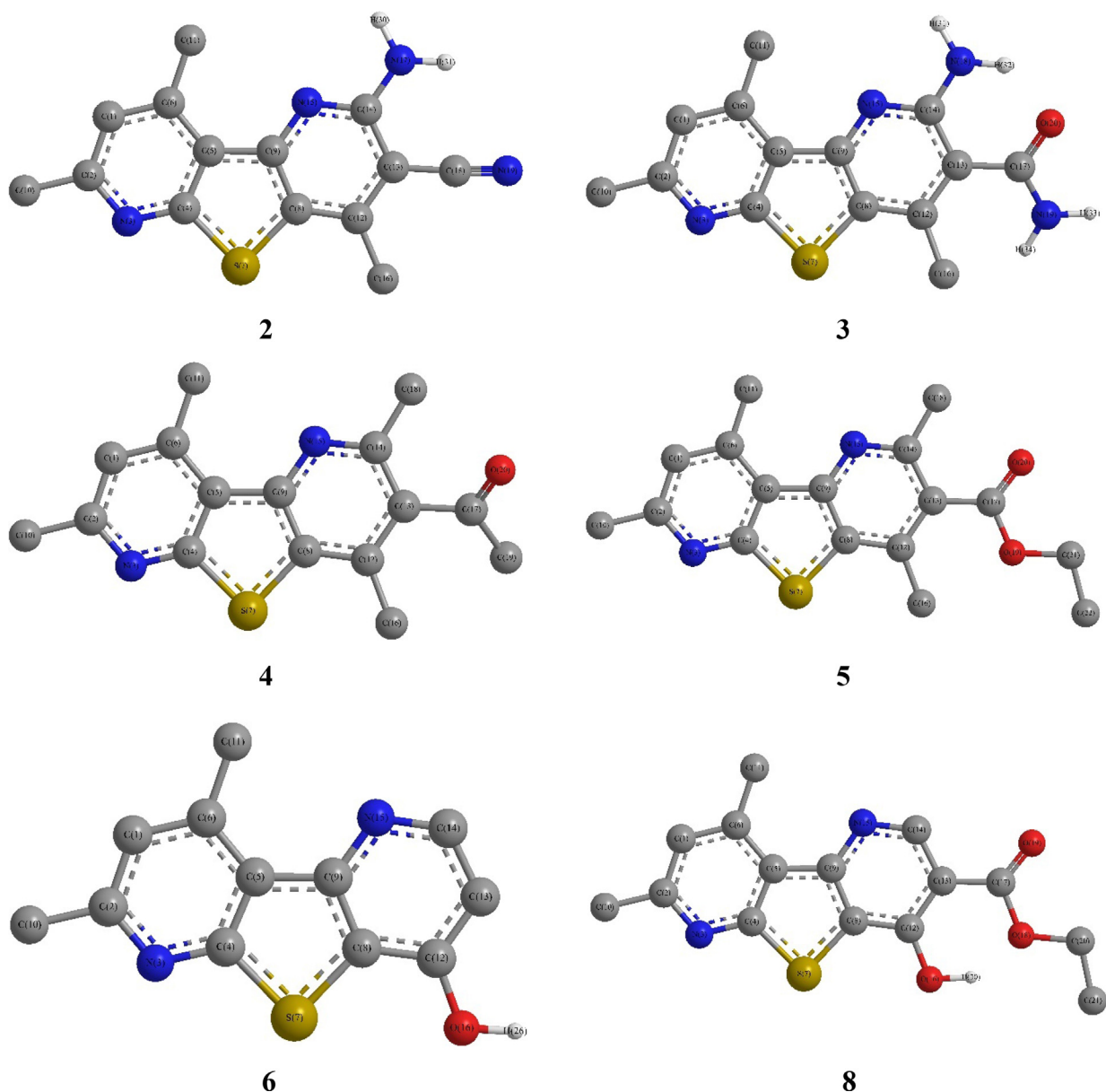


Fig. 3 Compounds 2–8 DFT Optimized structures.

and 0.013–0.158, that can be attached to their contribution in the fused rings resonance structure (Table 2). While, the negative charge of the sulfur atom,  $S_{(tpy)}^5$ , from  $-0.173$  to  $-0.730$ , cleared that its lone pairs of electrons did not participate in resonance of the thienodipyridine moiety. In addition, the carbon atom,  $C_{(tpy)}^2$ , in the amino derivatives 2–3, has more negative charge than in the methyl ones 4–5, which could be ascribed to the amino group electron release effect, but it has positive charge in derivatives 6–8. Also, the presence of 3-cyano substituent in compound 2 resulted in negative charge,  $-0.130$ , on the carbon atom  $C_{(tpy)}^3$  while it converted to be positive,  $0.146$ – $0.818$ , in the acetyl, amido and ester substituted derivatives 3–8. Correspondingly, the nitrogen and oxygen atoms of the substituents in all derivatives were negatively charged.

To explore the nucleophilic ( $f_k^+$ ) and electrophilic ( $f_k^-$ ) attacks susceptible sites, the Fukui's indices have been esti-

mated (Olasunkanmi et al., 2016, El Adnani et al., 2013, Mi et al., 2015, Messali et al., 2018). The inspected derivatives electrophilic attack indices ( $f_k^-$ ) showed that the thienodipyridine sulfur atom,  $S_{(tpy)}^5$ , has the maximum susceptibility while the amino nitrogen,  $NH_2$ , occupied the second position in compound 2 and 3. The hydroxy derivatives 6 and 8 presented coincided trend which is  $S_{(tpy)}^5 > C_{(tpy)}^2 > C_{(tpy)}^3 > OH$  while the methyl derivative 4 and 5 displayed different patterns (Table 3). Likewise, the radical attack indices ( $f_k^0$ ) data exhibited different patterns but the sulfur of thienodipyridine ( $S_{(tpy)}^5$ ) was the highest liable for radical attack in all compounds except in case of derivative 4 in which the first place was taken by acetyl oxygen atom ( $OC_{(Accl)}$ ) and then the thienodipyridine sulfur atom. Otherwise, the Fukui's indices ( $f_k^+$ ) demonstrated altered patterns where the  $S_{(tpy)}^5$  was the most susceptible site in case of 3, 5 and 6 derivatives while it

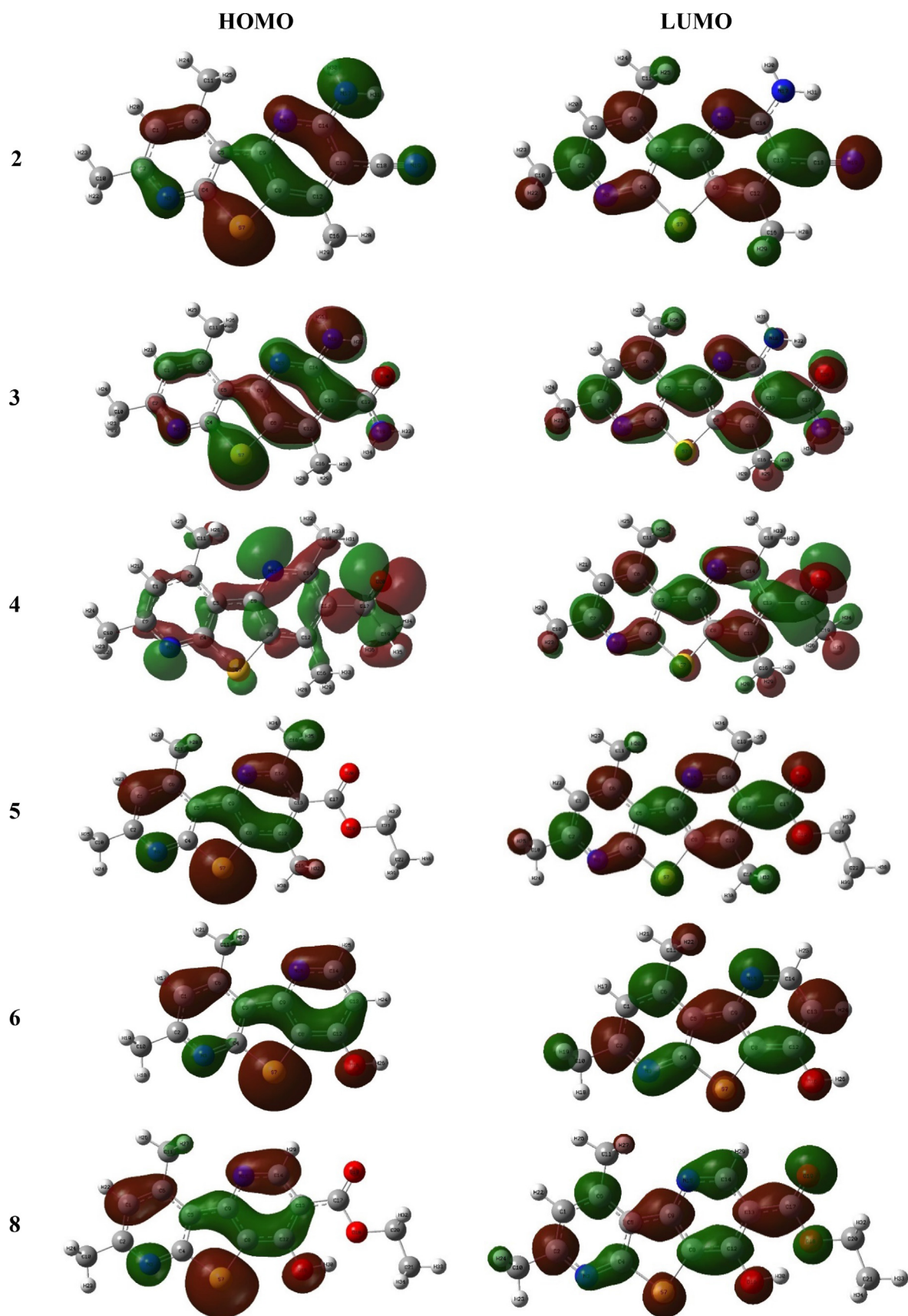


Fig. 4 The FMO plots of the compounds 2-8.

**Table 1** The studied thieno-dipyridine derivatives FMO energies and chemical reactivity descriptors (eV).

Compound	$E_H$	$E_L$	$\Delta E_{H-L}$	$\chi$	$\eta$	$\delta$	$\omega$	$\omega^+$	$\omega^-$
<b>2</b>	-6.05	-3.52	2.53	4.79	1.27	0.79	2.26	6.82	11.60
<b>3</b>	-5.67	-3.34	2.32	4.50	1.16	0.86	2.18	6.62	11.12
<b>4</b>	-6.39	-3.68	2.71	5.04	1.35	0.74	2.34	7.02	12.06
<b>5</b>	-6.40	-3.51	2.89	4.96	1.45	0.69	2.12	6.20	11.16
<b>6</b>	-6.30	-2.91	3.39	4.60	1.69	0.59	1.56	4.16	8.76
<b>8</b>	-6.43	-3.66	2.77	5.04	1.39	0.72	2.29	6.82	11.86

**Table 2** The Mulliken's charges of the studied thieno-dipyridine compounds (a.u.).

Atom	<b>2</b>	<b>3</b>	<b>4</b>	<b>5</b>	<b>6</b>	<b>8</b>
$N_{(tpy)}^1$	0.022	0.055	0.376	0.340	0.251	0.235
$C_{(tpy)}^2$	-0.816	-0.712	-0.364	-0.340	0.050	0.075
$C_{(tpy)}^3$	-0.130	0.750	0.801	0.397	0.146	0.818
$C_{(tpy)}^4$	0.964	0.824	0.709	0.926	0.965	0.912
$C_{(tpy)}^{4a}$	0.180	0.090	0.512	0.020	-0.876	-0.684
$S_{(tpy)}^5$	-0.379	-0.531	-0.421	-0.730	-0.173	-0.335
$C_{(tpy)}^{5a}$	-0.804	-0.764	-0.790	-0.144	-0.846	-0.759
$N_{(tpy)}^6$	0.158	0.124	0.142	0.013	0.093	0.093
$C_{(tpy)}^7$	0.892	0.818	0.724	0.252	0.525	0.505
$C_{(tpy)}^8$	-0.906	-0.939	-0.935	-0.624	-0.651	-0.762
$C_{(tpy)}^9$	0.722	0.824	0.613	0.741	0.916	0.920
$C_{(tpy)}^{9a}$	0.561	0.619	0.425	0.441	0.691	0.840
$C_{(tpy)}^{9b}$	-0.557	-0.382	-0.166	-0.265	-0.429	-0.164
$Me_{(tpy)}^7$	-0.864	-0.867	-0.857	-0.843	-0.905	-0.911
$Me_{(tpy)}^9$	-0.854	-0.837	-0.808	-0.805	-0.803	-0.855
$Me_{(tpy)}^4$	-0.953	-0.966	-0.769	-0.771		
$Me_{(tpy)}^2$			-0.876	-0.903		
NH <sub>2</sub>	-0.478	-0.643				
CN	0.014					
NC	-0.160					
CO <sub>(amd)</sub>		-0.424				
OC <sub>(amd)</sub>		-0.435				
NH <sub>2(amd)</sub>		-0.626				
CO <sub>(Actl)</sub>			-0.556			
OC <sub>(Actl)</sub>			-0.214			
Me <sub>(Actl)</sub>			-0.705			
CO <sub>(Estr)</sub>				-0.233		-0.221
O <sup>1</sup> C <sub>(Estr)</sub>				-0.264		-0.237
O <sup>2</sup> C <sub>(Estr)</sub>				-0.137		-0.190
CEt <sub>(Estr)</sub>				-0.097		-0.142
OH					-0.457	-0.462

appeared in the second position in **2** and **8** after cyano nitrogen (NC) and carboxylate oxygen ( $O^1C_{(Estr)}$ ) atoms, respectively. For instance, the amide derivative **3** displayed that  $S_{(tpy)}^5 > -OC_{(amd)} > C_{(tpy)}^7 > C_{(tpy)}^4$  while the derivative **5** exhibited another one,  $S_{(tpy)}^5 > O^1C_{(Estr)} > C_{(tpy)}^7 > C_{(tpy)}^{9a}$  (Table 3).

Occasionally, the Fukui's indices offered inaccurate in estimation probable sites for attack, therefore, the local relative electrophilicity and nucleophilicity descriptors,  $s_k^-/s_k^+$  and  $s_k^+/s_k^-$ , respectively, were computed (Roy et al., 1998b, Roy et al., 1998a, Roy et al., 1999), where  $\delta$  is global softness,  $s_k^+ = f_k^+ \times \delta$  and  $s_k^- = f_k^- \times \delta$ . The relative electrophilicity calculations,  $s_k^-/s_k^+$ , presented entirely diverse patterns than the

Fukui's indices. For example, the amino nitrogen, NH<sub>2</sub>, occupied the first position in case of **2-3** compounds, while in the other derivatives **4-8**, the fused ring sulfur atom,  $S_{(tpy)}^5$ , was the top one followed by the carbon  $C_{(tpy)}^2$  and  $C_{(tpy)}^8$  atoms in **4-5** and **6-8** derivatives, respectively. Likewise, the relative nucleophilicity,  $s_k^+/s_k^-$ , suggested other arrangements of the utmost vulnerable atoms. For instance, in compounds **2-4**, although they have thienodipyridine carbon atom,  $C_{(tpy)}^{9a}$ , as the most active site, their second place was captured differentially by cyano (CN), amide (CO<sub>(amd)</sub>), and acetyl (CO<sub>(Actl)</sub>) carbon atoms, respectively. Moreover, the other compounds **5** and **8** displayed close orders in which the carboxylate carbon

**Table 3** Selected electrophilic and nucleophilic reactivity indices of investigated thieno-dipyridine compounds.

2		3		4		5		6		8	
atom	$f_k^-$	atom	$f_k^-$	atom	$f_k^-$	atom	$f_k^-$	atom	$f_k^-$	atom	$f_k^-$
S <sub>(tpy)</sub> <sup>5</sup>	0.167	S <sub>(tpy)</sub> <sup>5</sup>	0.154	S <sub>(tpy)</sub> <sup>5</sup>	0.15	S <sub>(tpy)</sub> <sup>5</sup>	0.239	S <sub>(tpy)</sub> <sup>5</sup>	0.251	S <sub>(tpy)</sub> <sup>5</sup>	0.238
NH <sub>2</sub>	0.101	NH <sub>2</sub>	0.114	OC <sub>(ActI)</sub>	0.132	C <sub>(tpy)</sub> <sup>8</sup>	0.052	C <sub>(tpy)</sub> <sup>2</sup>	0.063	C <sub>(tpy)</sub> <sup>2</sup>	0.057
NC	0.084	C <sub>(tpy)</sub> <sup>4a</sup>	0.049	N <sub>(tpy)</sub> <sup>6</sup>	0.039	C <sub>(tpy)</sub> <sup>2</sup>	0.049	C <sub>(tpy)</sub> <sup>8</sup>	0.057	C <sub>(tpy)</sub> <sup>8</sup>	0.053
C <sub>(tpy)</sub> <sup>4a</sup>	0.047	N <sub>(tpy)</sub> <sup>1</sup>	0.047	C <sub>(tpy)</sub> <sup>2</sup>	0.039	N <sub>(tpy)</sub> <sup>6</sup>	0.044	OH	0.05	OH	0.049
2		3		4		5		6		8	
atom	$f_k^+$	atom	$f_k^+$	atom	$f_k^+$	atom	$f_k^+$	atom	$f_k^+$	atom	$f_k^+$
NC	0.109	S <sub>(tpy)</sub> <sup>5</sup>	0.067	OC <sub>(ActI)</sub>	0.101	S <sub>(tpy)</sub> <sup>5</sup>	0.071	S <sub>(tpy)</sub> <sup>5</sup>	0.09	O <sup>1</sup> C <sub>(Estr)</sub>	0.087
S <sub>(tpy)</sub> <sup>5</sup>	0.072	OC <sub>(amd)</sub>	0.063	CO <sub>(ActI)</sub>	0.079	O <sup>1</sup> C <sub>(Estr)</sub>	0.069	C <sub>(tpy)</sub> <sup>7</sup>	0.076	S <sub>(tpy)</sub> <sup>5</sup>	0.082
C <sub>(tpy)</sub> <sup>7</sup>	0.059	C <sub>(tpy)</sub> <sup>7</sup>	0.057	S <sub>(tpy)</sub> <sup>5</sup>	0.066	C <sub>(tpy)</sub> <sup>7</sup>	0.054	C <sub>(tpy)</sub> <sup>2</sup>	0.069	CO <sub>(Estr)</sub>	0.066
C <sub>(tpy)</sub> <sup>4</sup>	0.055	C <sub>(tpy)</sub> <sup>4</sup>	0.053	C <sub>(tpy)</sub> <sup>9b</sup>	0.049	C <sub>(tpy)</sub> <sup>9b</sup>	0.051	C <sub>(tpy)</sub> <sup>9</sup>	0.058	C <sub>(tpy)</sub> <sup>7</sup>	0.052
2		3		4		5		6		8	
atom	$f_k^0$	atom	$f_k^0$	atom	$f_k^0$	atom	$f_k^0$	atom	$f_k^0$	atom	$f_k^0$
S <sub>(tpy)</sub> <sup>5</sup>	0.119	S <sub>(tpy)</sub> <sup>5</sup>	0.111	OC <sub>(ActI)</sub>	0.116	S <sub>(tpy)</sub> <sup>5</sup>	0.155	S <sub>(tpy)</sub> <sup>5</sup>	0.171	S <sub>(tpy)</sub> <sup>5</sup>	0.16
NC	0.097	NH <sub>2</sub>	0.072	S <sub>(tpy)</sub> <sup>5</sup>	0.108	O <sup>1</sup> C <sub>(Estr)</sub>	0.05	C <sub>(tpy)</sub> <sup>7</sup>	0.054	O <sup>1</sup> C <sub>(Estr)</sub>	0.064
NH <sub>2</sub>	0.066	OC <sub>(amd)</sub>	0.049	CO <sub>(ActI)</sub>	0.057	C <sub>(tpy)</sub> <sup>7</sup>	0.042	C <sub>(tpy)</sub> <sup>3</sup>	0.054	C <sub>(tpy)</sub> <sup>2</sup>	0.048
C <sub>(tpy)</sub> <sup>7</sup>	0.046	N <sub>(tpy)</sub> <sup>1</sup>	0.047	C <sub>(tpy)</sub> <sup>9b</sup>	0.043	C <sub>(tpy)</sub> <sup>9b</sup>	0.042	C <sub>(tpy)</sub> <sup>2</sup>	0.052	OH	0.047
2		3		4		5		6		8	
atom	S <sup>+</sup> /S <sup>-</sup>	atom	S <sup>+</sup> /S <sup>-</sup>	atom	S <sup>+</sup> /S <sup>-</sup>	atom	S <sup>+</sup> /S <sup>-</sup>	atom	S <sup>+</sup> /S <sup>-</sup>	atom	S <sup>+</sup> /S <sup>-</sup>
C <sub>(tpy)</sub> <sup>9a</sup>	4.20	C <sub>(tpy)</sub> <sup>9a</sup>	5.00	C <sub>(tpy)</sub> <sup>9a</sup>	2.33	CO <sub>(Estr)</sub>	6.13	C <sub>(tpy)</sub> <sup>7</sup>	2.30	CO <sub>(Estr)</sub>	5.50
CN	2.69	CO <sub>(amd)</sub>	2.63	CO <sub>(ActI)</sub>	2.19	O <sup>2</sup> C <sub>(Estr)</sub>	3.43	C <sub>(tpy)</sub> <sup>9a</sup>	2.19	O <sup>2</sup> C <sub>(Estr)</sub>	3.86
C <sub>(tpy)</sub> <sup>4</sup>	2.04	C <sub>(tpy)</sub> <sup>9</sup>	2.15	C <sub>(tpy)</sub> <sup>4</sup>	1.88	O <sup>1</sup> C <sub>(Estr)</sub>	2.23	C <sub>(tpy)</sub> <sup>9</sup>	2.00	O <sup>1</sup> C <sub>(Estr)</sub>	2.12
C <sub>(tpy)</sub> <sup>9</sup>	1.96	C <sub>(tpy)</sub> <sup>7</sup>	1.84	C <sub>(tpy)</sub> <sup>7</sup>	1.53	C <sub>(tpy)</sub> <sup>5a</sup>	2.00	C <sub>(tpy)</sub> <sup>3</sup>	1.77	C <sub>(tpy)</sub> <sup>7</sup>	1.68
2		3		4		5		6		8	
atom	S <sup>-</sup> /S <sup>+</sup>	atom	S <sup>-</sup> /S <sup>+</sup>	atom	S <sup>-</sup> /S <sup>+</sup>	atom	S <sup>-</sup> /S <sup>+</sup>	atom	S <sup>-</sup> /S <sup>+</sup>	atom	S <sup>-</sup> /S <sup>+</sup>
NH <sub>2</sub>	3.37	NH <sub>2</sub>	3.68	S <sub>(tpy)</sub> <sup>5</sup>	2.27	S <sub>(tpy)</sub> <sup>5</sup>	3.37	S <sub>(tpy)</sub> <sup>5</sup>	2.79	S <sub>(tpy)</sub> <sup>5</sup>	2.90
C <sub>(tpy)</sub> <sup>4a</sup>	2.61	C <sub>(tpy)</sub> <sup>4a</sup>	3.06	C <sub>(tpy)</sub> <sup>2</sup>	1.70	C <sub>(tpy)</sub> <sup>2</sup>	1.96	C <sub>(tpy)</sub> <sup>8</sup>	1.63	C <sub>(tpy)</sub> <sup>8</sup>	1.83
S <sub>(tpy)</sub> <sup>5</sup>	2.32	S <sub>(tpy)</sub> <sup>5</sup>	2.30	C <sub>(tpy)</sub> <sup>4a</sup>	1.59	C <sub>(tpy)</sub> <sup>8</sup>	1.86	C <sub>(tpy)</sub> <sup>2</sup>	1.58	C <sub>(tpy)</sub> <sup>2</sup>	1.46
C <sub>(tpy)</sub> <sup>2</sup>	1.65	C <sub>(tpy)</sub> <sup>2</sup>	1.70	Me <sub>(tpy)</sub> <sup>2</sup>	1.36	Me <sub>(tpy)</sub> <sup>2</sup>	1.58	OH	1.28	N <sub>(tpy)</sub> <sup>1</sup>	1.29

presented on the top (CO<sub>(Estr)</sub>) and then the carboxylate oxygen atoms, O<sup>2</sup>C<sub>(Estr)</sub> and O<sup>1</sup>C<sub>(Estr)</sub>, in the 2nd and 3rd rank, respectively (Table 3).

In addition, the polarizability ( $\alpha_{\text{total}}$ ), hyperpolarizabilities ( $\beta_{\text{total}}$ ), and dipole moment ( $\mu$ ) are chief molecular parameters which evaluate the molecule's softness and electron density that mainly effects on intermolecular interactions (Aziz et al., 2022), as well as, optical nonlinearity and response (Shi, 2001, Prasad and Williams, 1991, Williams, 1984, Khan et al., 2021). The dipole moment ( $\mu$ ), polarizability ( $\alpha_{\text{total}}$ ) and first-order hyperpolarizability ( $\beta_{\text{total}}$ ) were described as (Sun et al., 2003, Abraham et al., 2008, Karamanis et al., 2008):

$$\mu = (\mu_x^2 + \mu_y^2 + \mu_z^2) \quad \alpha_{\text{total}} = \frac{(\alpha_{xx} + \alpha_{yy} + \alpha_{zz})}{3}$$

$$\beta_{\text{total}} = \sqrt{(\beta_{xxx} + \beta_{yyy} + \beta_{zzz})^2 + (\beta_{yyy} + \beta_{zzz} + \beta_{yxx})^2 + (\beta_{zzz} + \beta_{xxx} + \beta_{zyy})^2}$$

The examined compounds dipole moment ( $\mu$ ) was from 4.04 D, for compound 2, to 0.69 D, for compound 5. On comparison with urea ( $\mu = 1.3732$  Debye (Ahmed et al., 2008)), the derivatives 3 and 5 have lower dipole moment, 0.92 and

0.50 times, while other exhibited higher values, 1.21–2.94 times, which may be resulted from an overall charge inequality (Table 4). Moreover, the polarizability ( $\alpha_{\text{total}}$ ) data of the investigated derivatives displayed close values, where the derivative 5 and 6 exhibited the highest and lowest values,  $1.94 \times 10^{-23}$  and  $1.37 \times 10^{-23}$  esu, respectively, and can be arranged as  $6 < 2 < 3 < 8 < 4 < 5$ . Whereas, the first-order hyperpolarizability data of the studied compounds disclosed that the compound 2 has the higher value,  $\beta_{\text{total}} = 1.95 \times 10^{-30}$  esu, while 3 has the lowest,  $\beta_{\text{total}} = 3.62 \times 10^{-31}$  esu. (Table 4). On comparison with urea hyperpolarizability as reference material ( $\beta = 3.7389 \times 10^{-31}$  esu (Ahmed et al., 2008)), the data indicated that compound 3 and 2 were almost equal and greater than urea, 0.97 and 5.22 times, respectively.

### 3.3. Biological evaluation

#### 3.3.1. Antimicrobial activity

Using IZD and MIC techniques, the newly synthesized thieno-dipyridine derivatives were examined toward antibacterial effectiveness across Gram-positive and Gram-negative strains.

Fig. 5 established the antimicrobial behaviours of the synthesized analogues derivatives toward the antibacterial action because thienopyrimidines have the capability to block the construction of folic acid through both of the two bacterial strains (Wilding and Klempier, 2017). Over the investigated derivatives, they exhibited more reliable results against both “*S. aureus* and *B. subtilis*” Gram-positive and “*S. typhimurium* and *E. coli*” Gram-negative bacterial strains. Wherever, thieno-dipyridine analogues **2**, **3**, **5** and **8** nominated good activity as a general, especially toward Gram-positive bacteria rather than Gram-negative bacteria comparative to the results of ampicillin drug reference. Meanwhile, thieno-dipyridine derivative **2** have amino and nitrile groups displayed higher inhibition zone of (IZD = 26 mm, MIC = 18.52 µg/mL) against *S. aureus*, more than the reference ampicillin (IZD = 24 mm, MIC = 18.52 µg/mL). Likewise, thieno[2,3-*b*:4,5-*b'*]dipyridine derivative **3** have amino and carboxamide groups revealed (IZD = 21 mm, MIC = 18.52 µg/mL) against *B. subtilis* (Gram-positive) in comparison to the reference IZD = 22 mm, MIC = 18.52 µg/mL). Also, thieno-dipyridine derivative **5** have ethyl carboxylate ester moiety shown amazing inhibition against *S. aureus* with (IZD = 23 mm, MIC = 18.52 µg/mL). Whilst thieno-dipyridine derivative **8** has hydroxyl and ester groups exposed moderate inhibition against *S. aureus* with (IZD = 22 mm, MIC = 18.52 µg/mL).

Moreover, the results of hybrids **2**, **3**, **5** and **8** toward the Gram-negative bacteria “*S. typhimurium* and *E. coli*” were changed in their reactivity order. Derivatives **5** presented moral inhibition (IZD = 25 mm, MIC = 18.52 µg/mL) against *E. coli* more than the Ampicillin reference (IZD = 24 mm, MIC = 18.52 µg/mL). Whereas, derivatives **8** displayed moral inhibition (IZD = 23 mm, MIC = 18.52 µg/mL) against *S. typhimurium* equal to the reference (IZD = 23 mm, MIC = 18.52 µg/mL). Though, hybrid **2** revealed good inhibition (IZD = 21 mm, MIC = 18.52 µg/mL) against *E. coli*. Moreover, derivative **3** revealed (IZD = 20 mm, MIC = 18.52 µg/mL) against *S. typhimurium* (Table 5).

### 3.3.2. Structural activity relationship

Inspired by the interesting reactivity results of hybrids **2**, **3**, **5**, and **8** toward the four examined bacterial strains, most of the synthesized hybrids possess both hydrophilicity (from the polar moieties) and a hydrophobic effect from the existence of methyl groups, which increase their ability to penetrate

the bacterial cell membrane and increase their bacterial killing power. Though hybrid **2** displayed strong activity towards both *S. aureus* and *E. coli*, this was due to its polar moieties, such as amino and nitrile groups, in addition to its hydrophobic effect through its methyl group. Similarly, hybrid **3** showed equipotent reactivity towards both *B. subtilis* and *S. typhimurium*, indicating that it may contain polar moieties, such as amino and carboxamide groups, in addition to the three methyl groups. Meanwhile, Hybrid **5** revealed good reactivity towards *S. aureus* and eminent reactivity towards *E. coli*, according to its polar moieties like the ethyl carboxylate group in addition to four methyl groups. Moreover, hybrid **8** revealed reasonable reactivity towards *S. aureus* and equipotent reactivity towards *S. typhimurium*, indicating that it has polar moieties such as hydroxyl and ethyl carboxylate groups in addition to two methyl groups.

### 3.4. Molecular docking (MD)

Molecular docking is one of the most crucial techniques in structure-based drug design as it may provide an understanding of the novel molecules' modes of binding in the appropriate target's binding site, which is an essential stage in drug design (Mohi El-Deen et al., 2019; Nakamura et al., 2017). As the literary survey and PDB database were displayed the binding interactions with the thieno-pyridine derivatives for “*E. coli* DNA gyrase B” active site (PDB: 1AJ6), it was encouraged to inspect the binding affinity of the newly synthesized thieno[2,3-*b*:4,5-*b'*]dipyridine analogues towards (PDB code: 1AJ6) (Mohi El-Deen et al., 2019). In this study, MD studies were carried out to reveal the mechanism of binding between the novel bioactive chemical and the enzyme active binding site as well as any potential binding and the interaction score. Through the thieno-dipyridine system indicating their potential interactions inside “*E. coli* DNA gyrase B”, docking modeling was used to connect the experiential potencies and structural activity relationships (SAR) of newly created analogues. Table 6 contains the docking outcomes for the examined variants. Meanwhile, Derivative **2** was displayed two  $\pi$ -H bonds among Ile 78 and both of pyridine and thiophene rings through two bonds with length 4.50 and 3.86 Å, respectively. In addition, one H-acceptor between N19 of nitrile moiety with Gly 77 over docking score  $-5.5039$  Kcal/mol and root-mean square (RMSD) 0.8837 (Fig. S1). However, derivative **3** was revealed interaction between N3 of pyridine ring with His 99 amino-acid over H-acceptor, docking score

**Table 4** The dipole moment ( $\mu$ ), polarizability ( $\alpha_{\text{total}}$ ), polarizability anisotropy ( $\Delta\alpha$ ) and first-order hyperpolarizability ( $\beta_{\text{total}}$ ) of investigated compounds.

Compound	$\mu$ (Debye)	$\mu/\mu_{\text{urea}}$	$\alpha_{\text{total}}$ (esu $\times 10^{-23}$ )	$\Delta\alpha$ (esu $\times 10^{-24}$ )	$\beta_{\text{total}}$ (esu $\times 10^{-30}$ )	$\beta_{\text{total}}/\beta_{\text{urea}}$
<b>2</b>	4.04	2.94	1.77	3.31	1.95	5.22
<b>3</b>	1.27	0.92	1.78	6.24	0.36	0.97
<b>4</b>	1.82	1.32	1.84	5.37	0.83	2.22
<b>5</b>	0.69	0.50	1.94	5.99	0.49	1.32
<b>6</b>	3.16	2.30	1.37	4.28	0.91	2.43
<b>8</b>	1.66	1.21	1.80	7.28	1.09	2.91

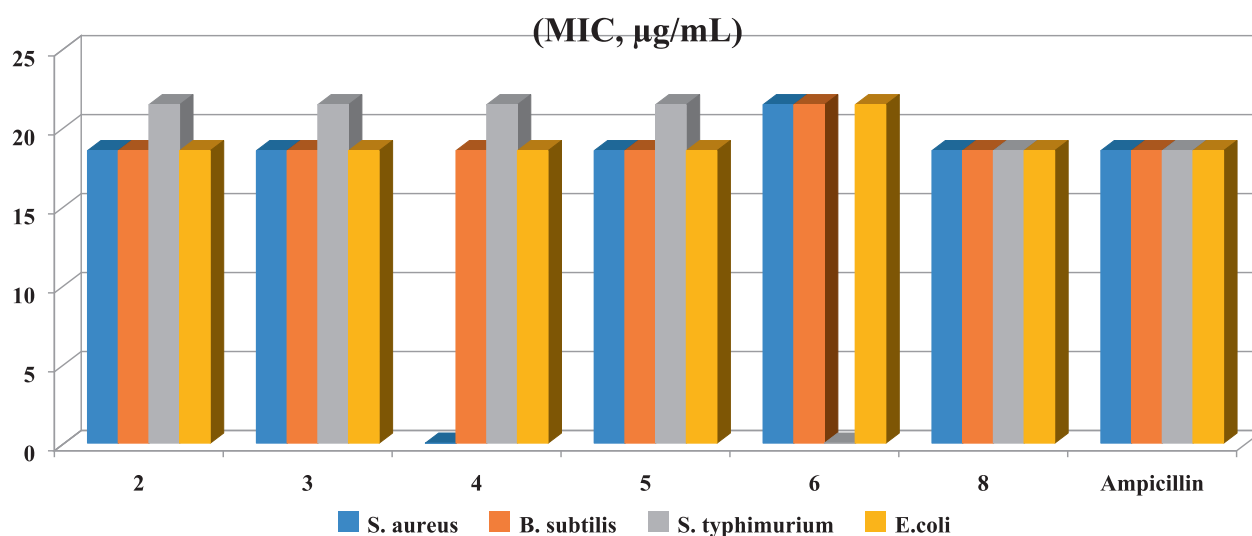


**Fig. 5** MIC of the examined derivatives toward both of Gram's positive and Gram's negative bacteria.

**Table 5** Inhibition zone and diameter (IZD mm) and minimum inhibition concentrations (MIC µg/mL) of the synthesized thieno[2,3-*b*:4,5-*b'*] dipyridine derivatives.

Organism	Gram-positive bacteria		Gram-negative bacteria	
	<i>S. aureus</i>	<i>B. subtilis</i>	<i>S. typhimurium</i>	<i>E. coli</i>
2	26 (18.52)	18(18.52)	16(21.43)	21(18.52)
3	20(18.52)	21(18.52)	20(21.43)	18(18.52)
4	NA	17(18.52)	15(21.43)	18(18.52)
5	23(18.52)	19(18.52)	19(21.43)	25(18.52)
6	16(21.43)	14(21.43)	NA	16(21.43)
8	18(18.52)	16(18.52)	23(18.52)	20(18.52)
Ampicillin	25(18.52)	22(18.52)	23(18.52)	24(18.52)

Notes: (IZD) inhibition zone diameter (mm), (MIC) minimum inhibition concentration (µg/mL), (NA) no activity, and Ampicillin is a standard antibiotic in case of Gram-positive bacteria, Cephalothin is a standard antibiotic in case of Gram-negative bacteria.

**Table 6** *In silico* docking consequences over thiophene and thienopyrimidine analogues.

Code	Docking score (S) (Kcal/mol)	RMSD (Refine unit)	ligand interactions	Interactions types	Distances (Å)
2	-5.5039	0.8837	N 19 with Gly 77 5-ring with Ile 78 6-ring with Ile 78	H-acceptor $\pi$ -H $\pi$ -H	3.11 4.50 3.86
3	-5.2587	1.3778	N 3 with His 99	H-acceptor	3.54
4	-5.0497	1.0430	S 7 with Asn 46	H-donor	3.18
5	-5.6385	0.9995	6-ring with Val 120	$\pi$ -H	4.57
6	-4.9306	1.1946	S 7 with Ala 100	H-donor	3.37
8	-5.5244	1.3913	6-ring with Val 120	$\pi$ -H	4.53
Ampicillin	-6.2245	1.3393	O 10 with Asn 46 O 16 with Val 120 6-ring with His 99	H-donor H-acceptor $\pi$ -H	2.92 3.22 3.57

−5.2587 Kcal/mol, RMSD = 1.3778, and bond length 3.54 Å (Fig. S2). Moreover, derivative 4 was exposed to interaction between S7 of thiophene ring with Asn 46 amino-acid over H-donor, RMSD = 1.0430, docking score −5.0497 Kcal/mol, and bond length 3.18 Å (Fig. S3). Though, derivative 5 was exhibited  $\pi$ -H interaction between pyridine ring with Val 120 of 1AJ6 amino-acid, highest docking score −5.6385 Kcal/mol, RMSD = 0.9995, and bond length 4.57 Å (Fig. 6).

Likewise, derivative 6 was H-donor interaction between S7 of thiophene ring with Ala 100 of amino-acid, lowest docking score −4.9306 Kcal/mol, RMSD = 1.1946, and bond length 3.37 Å (Fig. S4). Furthermore, derivative 8 was presented  $\pi$ -H interaction between pyridine ring with Val 120 of 1AJ6 amino-acid, acceptable docking score −5.5244 Kcal/mol, RMSD = 1.3913, and bond length 4.53 Å (Fig. 7).

Additionally, ampicillin was afforded H-donor between O 10 of carboxylic acid with Asn 46. H-acceptor bond among O 16 of urea moiety and Val 120, and  $\pi$ -H among benzene

moiety with His 99 over bond length 2.92, 3.22, and 3.57 Å, respectively, with score −6.2245 Kcal/mol, RMSD = 1.3393, (Fig. S5).

Finally, MD stimulation was pragmatic to endorse how far the synthesized thieno-dipyridine analogues interact as they bonded with many 1AJ6 amino-acids. Each of the six synthesized thieno-dipyridine analogues was reinforced by a network of  $\pi$ -H and H-bonds (H-doner, H-acceptor) with the N-atom and S-atom of both of pyridine and thiophene rings and chemical aromatic structures of thieno-dipyridines cooperate straight with 1AJ6 amino acids. The most of the synthesized thieno-dipyridine analogues had the 1AJ6 pocket, which were appeared as fork over polar and nonpolar residues of 1AJ6 amino acids (Gly 77, Ile 78, His 99, Asn 46, Val 120, and Ala 100). As well, the plurality of the thieno-dipyridine derivatives have the same amino acids, which is viewed as strong evidence for the effectiveness of the docking procedure.

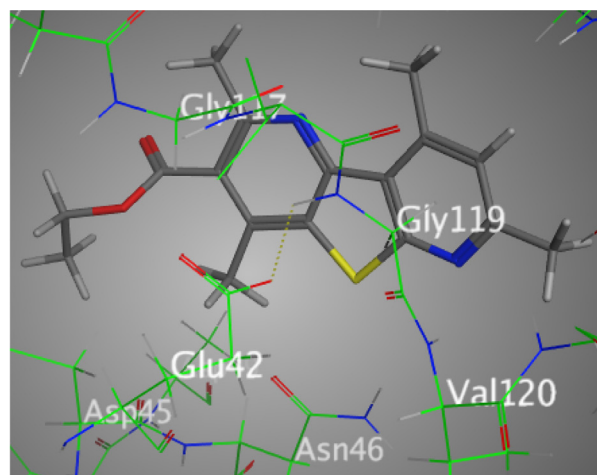
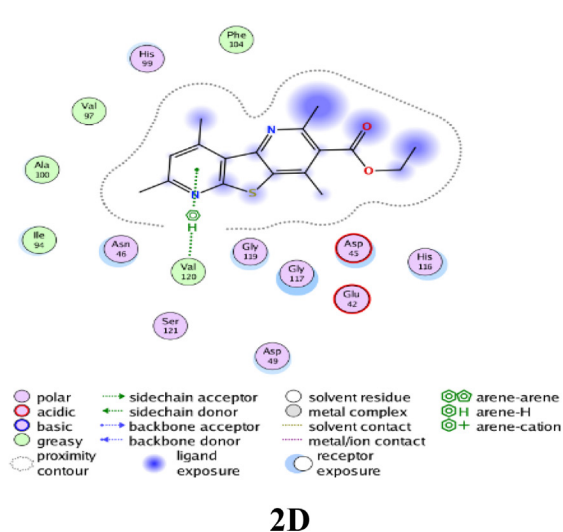


Fig. 6 Docking interactions over analogue 5 with 1AJ6.

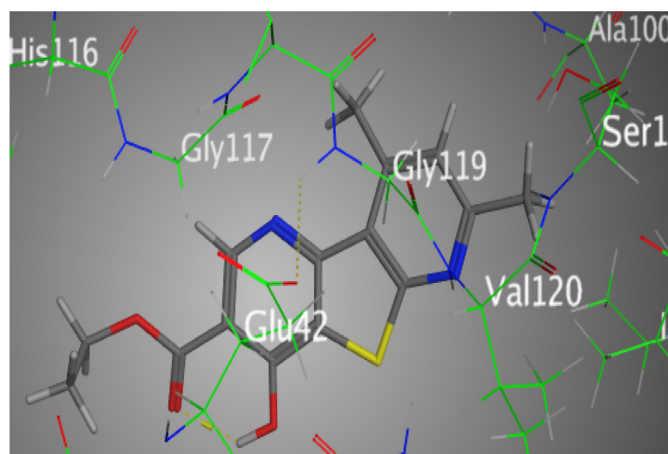
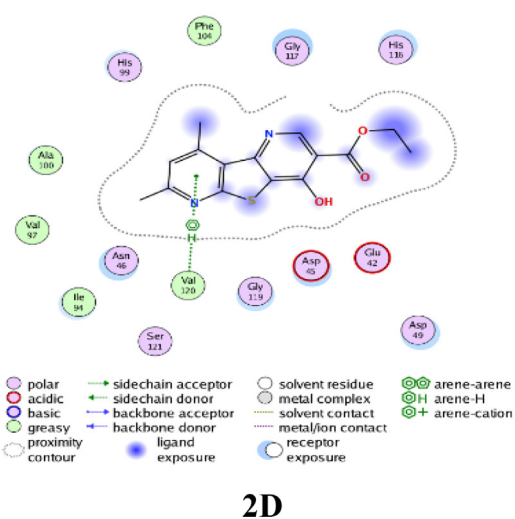


Fig. 7 Docking interactions over analogue 8 with 1AJ6.

#### 4. Conclusion

Six functionalized thieno[2,3-*b*:4,5-*b'*]dipyridine compounds obtained from the reactions of 2-acetyl-3-amino-4,6-dimethylthieno[2,3-*b*]pyridine with various active methylene reagents and/or DMF-DMA. The DFT studies of thieno-dipyridine derivatives revealed that the energy of FMO was affected by their configuration. The data indicated that the thienodipyridines, owing to their extended conjugation, exhibited low  $\Delta E_{H-L}$  gap and remarkable NLO properties. However, hybrids **2**, **3**, **5** and **8** designated good IZ and MIC toward Gram-positive bacteria (*S. aureus*, *B. subtilis*) with (IZ = 26, 21, 23, and 18 mm respectively, with MIC 18.52  $\mu\text{g/mL}$ ) rather than Gram-negative bacteria (*S. typhimurium*, *E. coli*), comparative to the results of ampicillin drug reference. Meanwhile, their structural activities relationship for the prepared analogues was discussed to explain the effect of their substituents on both of two Gram-positive and Gram-negative bacterial strains. Also, the molecular docking estimation was applied on these hybrids to inspect their binding interactions toward for *E. coli* DNA gyrase B active site (PDB code: 1AJ6). Moreover, the docking results showed agree to a reasonable degree with bacterial results of these derivatives toward *E. coli* bacteria.

#### Declaration of Competing Interest

The authors declare that they have no known competing financial interests or personal relationships that could have appeared to influence the work reported in this paper.

#### Acknowledgments

Princess Nourah bint Abdulrahman University Researchers Supporting Project number (PNURSP2023R122), Princess Nourah bint Abdulrahman University, Riyadh, Saudi Arabia.

#### Appendix A. Supplementary material

Supplementary material to this article can be found online at <https://doi.org/10.1016/j.arabjc.2023.104839>.

#### References

- Abraham, J.P., Sajan, D., Joe, I.H., Jayakumar, V., 2008. Molecular structure, spectroscopic studies and first-order molecular hyperpolarizabilities of *p*-amino acetanilide. *Spectrochim. Acta Part A: Mol. Biomol. Spectrosc.* 71, 355–367.
- Abuelhassan, S., Bakhite, E.A., Abdel-Rahman, A.E., El-Mahdy, A. F., Saddik, A.A., Marae, I.S., Abdel-Hafez, S.H., Tolba, M., 2022. Synthesis, photophysical properties, and biological activities of some new thienylpyridines, thienylthieno[2.3-*b*]pyridines and related fused heterocyclic compounds. *J. Heterocycl. Chem.* 60, 458–470.
- Adibpour, N., Khalaj, A., Rezaee, S., Daneshtalab, M., 2007. In vitro antifungal activity of 2-(4-substituted phenyl)-3 (2*H*)-isothiazolones. *Folia Microbiol.* 52, 573–576.
- Afolabi, S.O., Semire, B., Akiode, O.K., Idowu, M.A., 2022. Quantum study on the optoelectronic properties and chemical reactivity of phenoxazine-based organic photosensitizer for solar cell purposes. *Theor. Chem. Acc.* 141, 22.
- Ahmed, A.B., Feki, H., Abid, Y., Boughzala, H., Mlayah, A., 2008. Structural, vibrational and theoretical studies of *l*-histidine bromide. *J. Mol. Struct.* 888, 180–186.
- Al-Anazi, K.M., Mahmoud, A.H., Abulfarah, M., Allam, A.A., Fouda, M.M., Gaffer, H.E., 2019. 2-Amino-5-arylazothiazole-Based Derivatives. In *Vitro Cytotoxicity, Antioxidant Properties, and Bleomycin-Dependent DNA Damage*. *ChemistrySelect* 4, 5570–5576.
- Al-Mulla, A., 2017. A review: biological importance of heterocyclic compounds. *Der Pharma Chem.* 9, 141–147.
- Atta, A.M., Abdel-Latif, E., 2021. Synthesis and anticancer activity of new thiophene, thiazolyl-thiophene, and thienopyridine derivatives. *Russ. J. Gen. Chem.* 91, 456–463.
- Aziz, M., Ejaz, S.A., Tamam, N., Siddique, F., Riaz, N., Qais, F.A., Chtita, S., Iqbal, J., 2022. Identification of potent inhibitors of NEK7 protein using a comprehensive computational approach. *Sci. Rep.* 12, 1–17.
- Azoro, C., 2002. Antibacterial activity of Crude Extract of *Azadirachta indica* on *Salmonella typhi*. *World J. Biotechnol.* 3, 347–351.
- Bakhite, E.A., Abdel-Rahman, A.E., Al-Taifi, E.A., 2003. Synthesis of new thiopyridines, thienopyridines, pyridothienopyrimidines and pyranothienopyridines with anticipated biological activity. *J. Chem. Res.* 2003, 320–321.
- Becke, A.D., 1993. Density-functional thermochemistry. III. The role of exact exchange. *J. Chem. Phys.* 98, 5648–5652.
- Bhagyasree, J.B., Varghese, H.T., Panicker, C.Y., Samuel, J., Van Alsenoy, C., Bolelli, K., Yildiz, I., Aki, E., 2013. Vibrational spectroscopic (FT-IR, FT-Raman, <sup>1</sup>H NMR and UV) investigations and computational study of 5-nitro-2-(4-nitrobenzyl) benzoxazole. *Spectrochim. Acta A Mol. Biomol. Spectrosc.* 102, 99–113.
- Bhargava, S., Choudhary, A., Rathore, D., 2021. A Sustainable, Efficient, and Green Promoter for the Synthesis of Some Heterocyclic Compounds. *Emer. Trends Res. Chem. Sci.* Apple Academic Press.
- Biovia, D.S., 2017. *Materials Studio*. Dassault Systèmes, San Diego.
- Bouchoucha, A., Zaater, S., Bouacida, S., Merazig, H., Djabbar, S., 2018. Synthesis and characterization of new complexes of nickel (II), palladium (II) and platinum(II) with derived sulfonamide ligand: Structure, DFT study, antibacterial and cytotoxicity activities. *J. Mol. Struct.* 1161, 345–355.
- Bulat, F.A., Chamorro, E., Fuentealba, P., Toro-Labbe, A., 2004. Condensation of frontier molecular orbital Fukui functions. *J. Phys. Chem.* 108, 342–349.
- Delley, B., 2006. Ground-state enthalpies: evaluation of electronic structure approaches with emphasis on the density functional method. *J. Phys. Chem.* 110, 13632–13639.
- Dennington, R., Keith, T., Millam, J., 2009. *GaussView*, version 5. Semichem Inc., Shawnee Mission, KS.
- Domingo, L.R., Ríos-Gutierrez, M., Perez, P., 2016. Applications of the conceptual density functional theory indices to organic chemistry reactivity. *Molecules* 21, 748.
- El Adnani, Z., Mcharfi, M., Sfaira, M., Benzakour, M., Benjelloun, A., Touhami, M.E., 2013. DFT theoretical study of 7-*R*-3methylquinoxalin-2(1*H*)-thiones (RH; CH<sub>3</sub>; Cl) as corrosion inhibitors in hydrochloric acid. *Corros. Sci.* 68, 223–230.
- Fascio, M.L., Errea, M.I., D'accorso, N.B., 2015. Imidazothiazole and related heterocyclic systems. Synthesis, chemical and biological properties. *Eur. J. Med. Chem.* 90, 666–683.
- Felson, D.T., Smolen, J.S., Wells, G., Zhang, B., Van Tuyl, L.H., Funovits, J., Aletaha, D., Allaart, C.F., Bathon, J., Bombardieri, S., 2011. American College of Rheumatology/European League Against Rheumatism provisional definition of remission in rheumatoid arthritis for clinical trials. *Arthritis Rheumatism* 63, 573–586.
- Frisch, M., Trucks, G., Schlegel, H., Scuseria, G., Robb, M., Cheeseman, J., Scalmani, G., Barone, V., Mennucci, B., Petersson, G., 2009. *Gaussian 09W*. Revision A. Gaussian, Inc., Wallingford, CT, USA.
- Istanbullu, H., Bayraktar, G., Saylam, M., 2022. Fused Pyridine Derivatives: Synthesis and Biological Activities, Exploring Chemistry with Pyridine Derivatives. *IntechOpen*.
- Karamanis, P., Pouchan, C., Maroulis, G., 2008. Structure, stability, dipole polarizability and differential polarizability in small gallium

- arsenide clusters from all-electron ab initio and density-functional-theory calculations. *Phys. Rev.* 77, 013201.
- Kaushal, M., Lobana, T.S., Nim, L., Kaur, J., Bala, R., Hundal, G., Arora, D.S., Garcia-Santos, I., Duff, C.E., Jasinski, J.P., 2018. Synthesis, structures, antimicrobial activity and biosafety evaluation of pyridine-2-formaldehyde-N-substituted-thiosemicarbazones of copper (II). *New J. Chem.* 42, 15879–15894.
- Khan, M.U., Khalid, M., Shafiq, I., Khera, R.A., Shafiq, Z., Jawaria, R., Shafiq, M., Alam, M.M., Braga, A.A.C., Imran, M., 2021. Theoretical investigation of nonlinear optical behavior for rod and T-Shaped phenothiazine based D- $\pi$ -A organic compounds and their derivatives. *J. Saudi Chem. Soc.* 25, 101339.
- Klemm, L.H., Weakley, T.J., Yoon, M., Clegg, R.S., 2000. A comparison of crystallographic and NMR data for thieno[2,3-*b*:4,5-*b'*]dipyridine and its monohydroperchlorate salt. *J. Heterocycl. Chem.* 37, 763–766.
- Koller, M., Carcache, D.A., Orain, D., Ertl, P., Behnke, D., Desrayaud, S., Laue, G., Vranesic, I., 2012. Discovery of 1*H*-pyrrolo[2,3-*c*]pyridine-7-carboxamides as novel, allosteric mGluR5 antagonists. *Bioorg. Med. Chem. Lett.* 22, 6454–6459.
- Lee, C., Yang, W., Parr, R.G., 1988. Development of the Colle-Salvetti correlation-energy formula into a functional of the electron density. *Phys. Rev. B* 37, 785–789.
- Makhlouf, M.M., Radwan, A.S., Ghazal, B., 2018. Experimental and DFT insights into molecular structure and optical properties of new chalcones as promising photosensitizers towards solar cell applications. *Appl. Surf. Sci.* 452, 337–351.
- Messali, M., Larouj, M., Lgaz, H., Rezki, N., Al-Blewi, F., Aouad, M., Chaouiki, A., Salghi, R., Chung, I.M., 2018. A new schiff base derivative as an effective corrosion inhibitor for mild steel in acidic media: Experimental and computer simulations studies. *J. Mol. Struct.* 1168, 39–48.
- Mi, H., Xiao, G., Chen, X., 2015. Theoretical evaluation of corrosion inhibition performance of three antipyrine compounds. *Comput. Theor. Chem.* 1072, 7–14.
- Mohamed, Y.M., Solum, E.J., Eweas, A.F., 2018. Synthesis, antibacterial evaluation, and docking studies of azaisoflavone analogues generated by palladium-catalyzed cross coupling. *Monatsh. Chem.* 149, 1857–1864.
- Mohi El-Deen, E.M., Abd El-Meguid, E.A., Hasabelnaby, S., Karam, E.A., Nossier, E.S., 2019. Synthesis, docking studies, and in vitro evaluation of some novel thienopyridines and fused thienopyridine-quinolines as antibacterial agents and DNA gyrase inhibitors. *Molecules* 24, 3650.
- Nakamura, R.L., Burlingame, M.A., Yang, S., Crosby, D.C., Talbot, D.J., Chui, K., Frankel, A.D., Renslo, A.R., 2017. Identification and optimization of thienopyridine carboxamides as inhibitors of HIV regulatory complexes. *Antimicrob. Agents Chemother.* 61, e02366–e02416.
- Naushad, E., Thangaraj, S., 2022. Naturally isolated pyridine compounds having pharmaceutical applications. *Exploring chemistry with pyridine derivatives*. IntechOpen.
- Olasunkanmi, L.O., Obot, I.B., Ebenso, E.E., 2016. Adsorption and corrosion inhibition properties of N-{*n*-[1-*R*-5-(quinoxalin-6-yl)-4,5-dihydropyrazol-3-yl] phenyl} methanesulfonamides on mild steel in 1 M HCl: experimental and theoretical studies. *RSC Adv.* 6, 86782–86797.
- Perdew, J.P., Wang, Y., 1992. Pair-distribution function and its coupling-constant average for the spin-polarized electron gas. *Phys. Rev.* 46, 12947–12954.
- Prasad, P.N., Williams, D.J., 1991. *Introduction to nonlinear optical effects in molecules and polymers*. Wiley, New York.
- Rodinovskaya, L., Shestopalov, A., 2000. Synthesis of substituted 4-hydroxy-1*H*-thieno[2,3-*b*; 4,5-*b'*]dipyridin-2-ones. *Russ. Chem. Bull.* 49, 348–354.
- Roy, R., De Proft, F.D., Geerlings, P., 1998a. Site of protonation in aniline and substituted anilines in the gas phase: a study via the local hard and soft acids and bases concept. *J. Phys. Chem.* 102, 7035–7040.
- Roy, R., Krishnamurti, S., Geerlings, P., PaL, S., 1998b. Local softness and hardness based reactivity descriptors for predicting intra- and intermolecular reactivity sequences: carbonyl compounds. *J. Phys. Chem.* 102, 3746–3755.
- Roy, R.K., Pal, S., Hirao, K., 1999. On non-negativity of Fukui function indices. *J. Chem. Phys.* 110, 8236–8245.
- Sajan, D., Joseph, L., Vijayan, N., Karabacak, M., 2011. Natural bond orbital analysis, electronic structure, non-linear properties and vibrational spectral analysis of L-histidinium bromide monohydrate: a density functional theory. *Spectrochim. Acta Part A: Mol. Biomol. Spectrosc.* 81, 85–98.
- Shi, Y., 2001. Particle swarm optimization: developments, applications and resources. In: *Proceedings of the 2001 congress on evolutionary computation (IEEE Cat. No. 01TH8546)*. IEEE, pp. 81–86.
- Sun, Y., Chen, X., Sun, L., Guo, X., Lu, W., 2003. Nanoring structure and optical properties of Ga8As8. *Chem. Phys. Lett.* 381, 397–403.
- Sun, Y., Gu, Y., Yang, J., 2022. Adsorption of N-heterocyclic compounds from aqueous solutions by sulfonic acid-functionalized hypercrosslinked resins in batch experiments. *Chem. Eng. J.* 428, 131163.
- Tevyashova, A.N., Chudinov, M.V., 2021. Progress in the medicinal chemistry of organoboron compounds. *Russ. Chem. Rev.* 90, 451.
- Ul-Haq, Z., Khan, A., Ashraf, S., Morales-Bayuelo, A., 2020. Quantum mechanics and 3D-QSAR studies on thienopyridine analogues: inhibitors of IKK $\beta$ . *Heliyon* 6, e04125.
- Wilding, B., Klempier, N., 2017. Newest developments in the preparation of thieno[2,3-*d*]pyrimidines. *Org. Prep. Proced. Int.* 49, 183–215.
- Williams, D.J., 1984. Organic polymeric and non-polymeric materials with large optical nonlinearities. *Angew. Chem. Int. Ed. Engl.* 23, 690–703.
- Xavier, S., Periandy, S., Ramalingam, S., 2015. NBO, conformational, NLO, HOMO–LUMO, NMR and electronic spectral study on 1-phenyl-1-propanol by quantum computational methods. *Spectrochim. Acta Part A: Mol. Biomol. Spectrosc.* 137, 306–320.
- Yassin, F., 2009. Synthesis, reactions and biological activity of 2-substituted 3-cyano-4, 6-dimethylpyridine derivatives. *Chem. Heterocycl. Compd.* 45, 35–41.